SUPERCONDUCTING DC AND RF PROPERTIES OF INGOT NIOBIUM

Pashupati Dhakal#, Gianluigi Ciovati, Peter Kneisel, and Ganapati Rao Myneni

Jefferson Lab, Newport News, VA

ABSTRACT

The thermal conductivity, DC magnetization and penetration depth of large-grain niobium hollow cylindrical rods fabricated from ingots, manufactured by CBMM subjected to chemical and heat treatment were measured. The results confirm the influence of chemical and heat-treatment processes on the superconducting properties, with no significant dependence on the impurity concentrations in the original ingots. Furthermore, RF properties, such as the surface resistance and quench field of the niobium rods were measured using a TE_{011} cavity. The hollow niobium rod is the center conductor of this cavity, converting it to a coaxial cavity. The quench field is limited by the critical heat flux through the rods' cooling channel.

Introduction

Table1. Contents ppm (per weight) of the main interstitial impurities from the different Nb ingots and RRR obtained from the samples' thermal conductivity at 4.2 K measured "as machined"

Samples	Ta	H	O	N	C	RRR
F	1330	<1	<6	<3	<30	226±10
G	1375	7.1	<6	<3	<30	197± 8
H	704	<1	<6	<3	<30	240± 9
I	708	5.4	<6	<3	<30	224±8

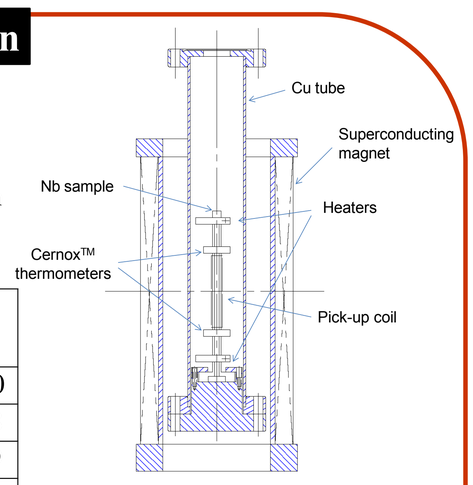

Fig.1 Experimental setup, a system to measure the magnetization curve, the thermal conductivity, the penetration depth and the surface pinning characteristics of the sample rod.

Sample Preparation

- Cylindrical hollow rod with one end closed of 12cm long, 12 mm OD and 8 mm ID from CBMM (as machined)
- 100 μm BCP 1:1:2
- Heat treatment at 800 C/3hrs + 140 C/3hrs

Magnetization and Penetration depth

The induced voltage is measured as a function of applied magnetic field and the DC magnetization is calculated as

$$M(H_e) = \frac{1}{1-N_d}\int_0^{H_e} \frac{V(H) - V_n}{V_s - V_n} dH$$

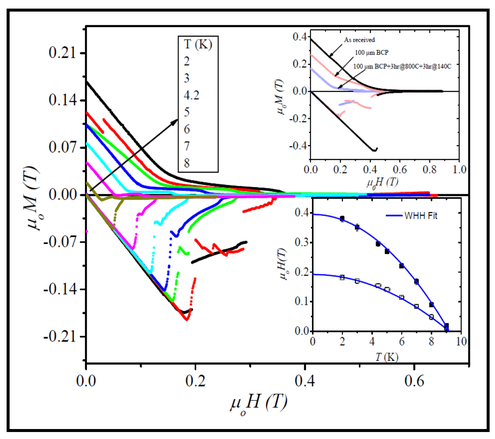

Fig. 4: The magnetization measurements carried out in the temperature range 2-8K of sample-I

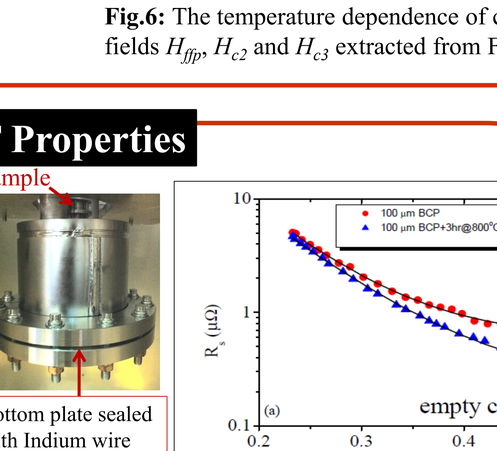

Fig. 5 The change in resonant frequency of LC oscillator with external magnetic field

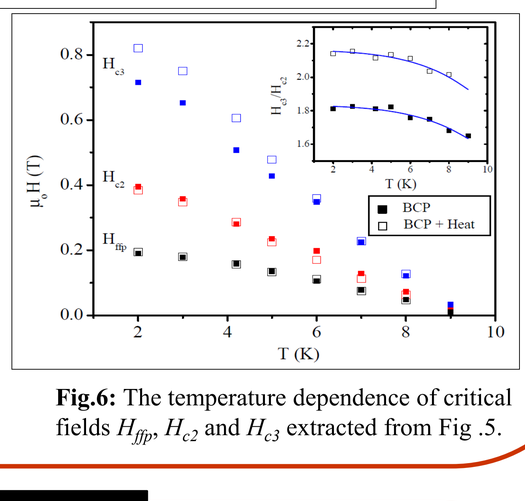

Fig.6: The temperature dependence of critical fields H_{ffp}, H_{c2} and H_{c3} extracted from Fig .5.

Thermal Conductivity and Transition Temperature

The total thermal conductivity of a superconductor is sum of the electronic conduction due to the unpaired electrons and lattice thermal conductivity as

$$\kappa(T) = \kappa_e(T) + \kappa_{ph}(T) = R(y)\left[\frac{\rho}{LT} + AT^2\right]^{-1} + \left[\frac{1}{DT^2 e^{y}} + \frac{1}{BlT^3}\right] \quad \ldots\ldots (1)$$

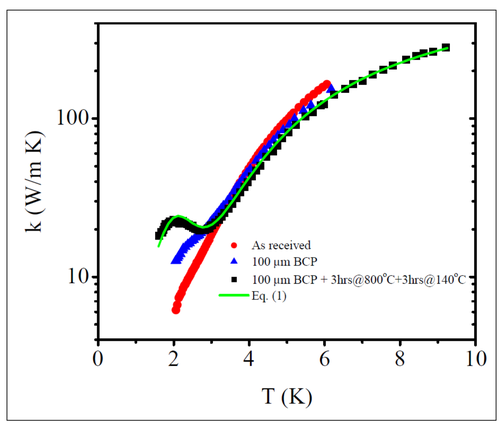

Fig. 2 The temperature dependence of thermal Conductivity of sample-I after various treatments. The solid line is the fit using Eq.(1)

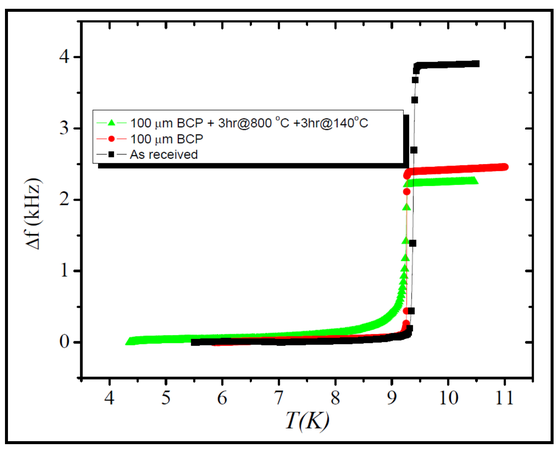

Fig. 3 The change in resonant frequency of LC oscillator with temperature showing the sharp transition when the sample–H goes superconducting to normal state.

The transition temperature for as machined sample is 9.35±0.02K, where as BCP and heat treatments sample has T_c = 9.25±0.02 K.

RF Properties

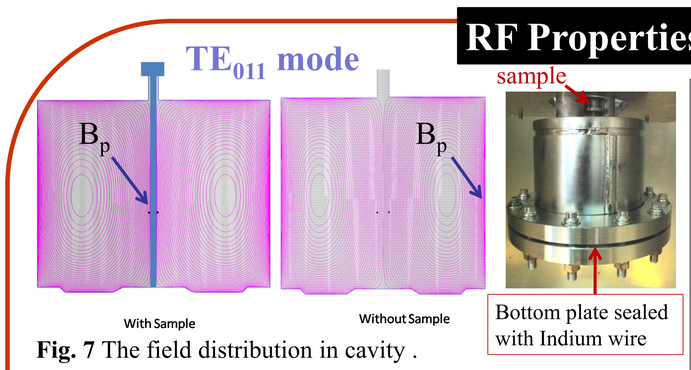

Fig. 7 The field distribution in cavity .

$B_{p,sample} = 2.2\ B_{p,cavity}$ $\quad P_{sample}/R_s = 0.3\ P_{cav}/R_s$

Parameters	Empty	w. sample
Resonant frequency (GHz)	3.501	3.856
Bp/√U (mT/J)	62.7	114.2
Geometric factor ($G = Q_0 R_s$)	779.6 Ω	532.2 Ω

Figure 9: The power dissipation in the sample as a function of peak RF field for sample-H

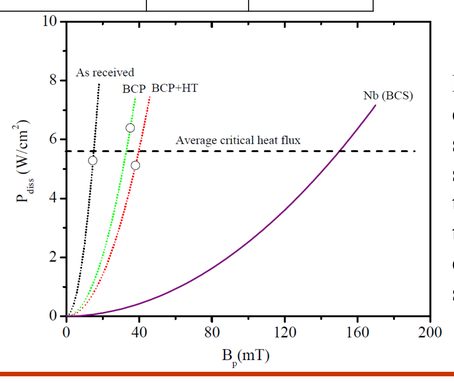

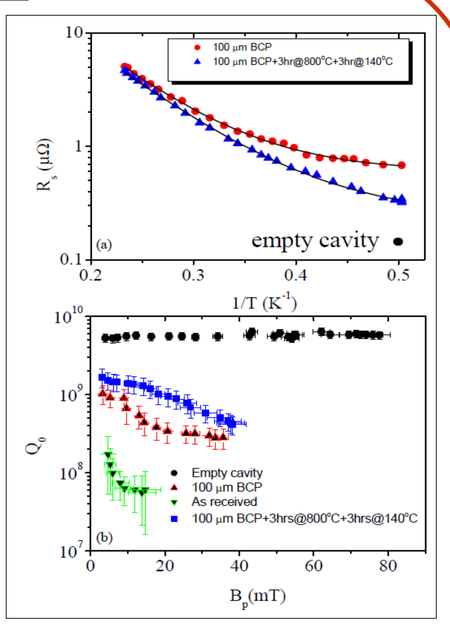

Fig. 8: Summary of the RF test on the TE_{011} cavity. (a) The temperature dependence of surface resistance of TE_{011} coaxial cavity with sample H after BCP and BCP followed by heat treatment at B_p = 5.5 mT. The solid lines are the fits using BCS codes (b) The Q_0 of the cavity in "pill-box" and coaxial geometry with sample–H at 2K.

Conclusions and Future Works

- 2K phonon peak in thermal conductivity due to the high temperature (HT) treatment.
- Improvement of surface critical field due to HT and low temperature baking (LTB).
- RF measurement on TE_{011} cavity shows the reduction of surface resistance and hence the increase in quality factor due to the chemical and heat treatment, however maximum peak magnetic field is limited due to the critical heat flux of the niobium rods.
- The further chemical treatment (EP), longer LTB and several combination of chemical and heat treatment are planned for future work in understanding the limiting factors of cavity performance and implementation of these results to new generation SRF cavities.

Acknowledgements

We would like to acknowledge P. Kushnick and M. Morrone at Jefferson Lab for the technical support. This is authored by Jefferson Science Associates, LLC under U.S. DOE Contract No. DE-AC05-06OR23177. The U.S. Government retains a non-exclusive, paid-up, irrevocable, world-wide license to publish or reproduce this manuscript for U.S. Government purposes.

dhakal@jlab.org

Jefferson Lab
Thomas Jefferson National Accelerator Facility